Formation and Reversion of Stress Induced Martensite in Ti-10V-2Fe-3Al

Duerig, Albrecht, Richter, Fischer

Acta metall
Vol. 30
pp. 2161-2172

1982

Acta metall. Vol. 30, pp. 2161 to 2172, 1982
Printed in Great Britain.

0001-6160/82/122161-12$03.00/0

FORMATION AND REVERSION OF STRESS INDUCED MARTENSITE IN Ti–10V–2Fe–3Al

T. W. DUERIG[1], J. ALBRECHT[1], D. RICHTER[2] and P. FISCHER[3]

[1]Brown Boveri Research Center, CH-5405 Baden,
[2]Battelle Research Center, CH-1227 Geneva and
[3]Institut für Reaktortechnik, CH-5305 Würenlingen, Switzerland

(*Received* 13 *May* 1982)

Abstract—The formation and reversion behavior of stress induced orthorhombic martensite (α'') in Ti–10V–2Fe–3Al has been studied, and several interesting features found. Reversion appears to take place in four stages. First, there is an athermal reshearing of α'' back to the b.c.c. parent phase, which is accompanied by a significant one-way shape memory effect between 165° and 240°C. This athermal reversion competes with an isothermal stabilization of the α'' plates. Further heating results in the isothermal precipitation of α, which seems to reproduce the preferred orientations of the previous α'', and is thus also accompanied by a shape memory effect; an isothermal shape memory effect in the opposite direction as the preceeding athermal shape change. The precipitation of α occurs on two microstructural scales, extremely fine α nucleating in the β matrix on extant isothermal ω particles, and the direct transformation of the unreverted α'' plates to α. Finally, when heating is continued to the β-transus temperature, the α begins to dissolve back to the parent β. This final dissolution is accompanied by a textural loss in the α phase, and consequently gives rise to several final "shape adjustments", the nature of which have not been fully explained.

Résumé—On a etudié la formation et le comportement reversible de martensite orthorombique produite par des contraintes, dont on a trouvé quelques aspects intéréssants. Il semble que la reversion a lieu en quatre étapes. Premièrement, il y a un recisaillement athermique de α'' dans la phase originale b.c.c., qui est accompagné par un considérable effet de mémoire unidirectionel entre 165° et 240°C. Cette reversion athermique est en compétition avec une stabilization isothermique des lâmes de α''. La continuation du chauffement produit la précipitation isothermique de α, qui semble reproduire les orientations preferentielles de la phase α'' antérieure, et qui devient donc accompagné par un effet de mémoire, cet effet ci dans le sens opposé au précedent effect athermique. La précipitation de α a lieu à deux niveaux microstructurels, d'une part la nucléation de α extrèment fine dans la matrice β, aux particules ω pré-existantes, et d'autre part la transformation directe des lâmes α'' pas changeés, en α. Finalement, si l'on continue le chauffement jusqa'à la temperature β-transus, α commence a se dissoudre de nouvean au β entourant. Cette dissolution finale est accompagneé par une perte de texture à la phase α, et par conséquence produit quelques "mises an point" de forme finales, dont la nature n'a pas encore été complètement expliquée.

Zusammenfassung—Die Untersuchung der Bildung und Rückumwandlung des spannungsinduzierten, orthorhombischen Martensit (α'') in Ti–10V–2Fe–3Al erbrachte einige interessante Ergebnisse. Demnach erfolgt die Rückbildung in vier Stufen. Der erste Schritt ist die athermische Rückscherung des α'' zur raumzentrierten Ausgangsphase (β), begleitet von einem beträchtlichen Einweg-Formgedächtniseffekt zwischen 165° und 240°C. Diese athermische Rückbildung verläuft in Konkurrenz mit einer isothermen Stabilisierung der α''-Lamellen. Weiteres Aufheizen bewirkt eine isothermische Ausscheidung der α-Phase, die die bevorzugte Orientierung des vormaligen α'' zu reproduzieren scheint und daher begleitet wird von einem isothermen Formgedächtniseffekt in entgegengesetzter Richtung zum vorhergehenden athermischen Gedächtniseffekt. Die Ausscheidung von α findet statt auf zwei mikrostrukturellen Grössenebenen: extrem feine α-Ausscheidungen, die die isothermen ω-Teilchen ersetzen und direkte Umwandlung der nicht-rückgebildeten α''-Lamellen in α. Wird schliesslich das Aufheizen bis zur β-Transus-Temperatur fortgesetzt, beginnt sich die α-Phase in die β-Hochtemperaturphase aufzulösen. Durch diese Auflösung geht die Textur der α-Phase verloren, was folglich zu verschiedenen, abschliessenden "Formanpassungen" Anlass gibt, deren Natur noch nicht vollständig verstanden ist.

INTRODUCTION

Stress induced, or stress assisted, martensitic transformations have now been reported in a broad range of experimental and commercial titanium alloys. Early studies of the structural nature of these martensites indicated a variety of possible structures, including h.c.p. [1, 2], b.c.c. [3], and the hexagonal omega structure [4]. More recent studies, however, indicate that these stress induced phases are generally orthorhombic [5–8]. Williams [9], in fact, has concluded that all stress induced martensites are orthorhombic, (designated α''), and that these earlier structural identifications were based on experimental techniques of insufficient accuracy to resolve the orthorhombic structure.

Athermal orthorhombic martensites, meaning martensites precipitating on quenching without the assistance of an external stress, have also been reported in a variety of Ti alloy systems [6, 10–16]. Although detailed studies of the structure of these martensites have been largely hampered by thin foil relaxation effects [17], there are some well-founded conclusions one can draw from the literature. As the stability of the transforming matrix is increased, either chemically or by heat treatment, there is an increasing tendency to form the orthorhombic structure in preference to the hexagonal structure, the cut-off in the Ti–Mo system, for example, being 4 wt% Mo [9, 11, 14]. The orientation relationship between the original β and the sheared α'' orthorhombic phase has been established approximately as

$$(110)_\beta \parallel (001)_{\alpha''}$$

$$[111]_\beta \parallel [101]_{\alpha''}.$$

Transformation strains from the $\beta \rightarrow \alpha''$ transformation seem to be accommodated primarily by internal twinning on the $\{111\}_{\alpha''}$ planes, in contrast to the hexagonal martensites which tend to exhibit a heavily damaged internal structure. In alloy systems exhibiting compositionally invariant decompositions of β into both the α'' and the ω structures, it has not been determined with any certainty what the correlation between the two new phases is, though it has been speculated [7] that the ω particles could be sheared along with the surrounding β into the new α'' structure.

Several modes of reversion, or tempering, have been reported to exist in athermal α'' (not stress induced), and have been reviewed by many authors [9, 11, 12]. The exact mechanics of the reversion process seem to be dependent on the details of the alloy system being studied. Bagariatskii [14], for example, reported a solute enrichment of α'' coincident with internal α precipitation, eventually leading to decomposition to the equilibrium $\alpha + \beta$ structure. Williams and Hickman [10] reported the precipitation of fine α needles within the α'' plates in a Ti–4% Mo–0.25% Si alloy. In the commercial Ti–6–2–4–6 alloy, Young *et al.* [15] have reported a loss of orthorhombicity coupled with the homogeneous precipitation of Burger's oriented α as being the first step of reversion. Davis *et al.* [12, 13] have reported a spinodal decomposition of the α'' plates in a variety of the Ti–Mo compositions. Finally, in alloys with M_s temperatures near room temperature (as is the case with systems exhibiting stress induced transformations), the α'' plates have been thought to form β by an athermal reshearing mechanism [9, 16].

Baker [6] has studied the reversion behavior of a deformed Ti–35 wt% Nb alloy, and found that the reversion of α'' to β was associated with a shape memory effect. What made this observation somewhat unique is that the parent β phase was not ordered. Ordering of the parent phase (as is found in NiTi and the β-brass memory alloys) had been thought to be one of the prime prerequisites of a shape memory effect [17, 18]. The benefit of having an ordered parent, or austenitic, phase is that the martensite gives preference to reversion to the original austenite variant, since only the original austenite variant restores the crystal ordering as it was prior to deformation.

The metastable β–Ti alloy Ti–10V–2Fe–3Al is a commercial alloy in which the BCC β structure is sufficiently stabilized by Fe and V additions to allow the high temperature β phase to be completely retained during a rapid quench from the alloy's 800°C β-transus temperature. The stability of the alloy is insufficient, however, to prevent it from martensitically decomposing when a sufficient external stress is applied [7]. A previous study of this stress assisted transformation confirmed that the martensitic structure was orthorhombic, and that the stress needed to induce the transformation was about 250 MPa [7]. The purpose of this paper will be to report on the unusual reversion behavior of the stress induced products of this alloy, and to discuss the attendant shape memory effects [19]. A later paper will discuss the effects of the stress assisted transformation on various mechanical properties, emphasizing crack growth studies.

EXPERIMENTAL

Although six heats of material were investigated in this study, the material used for the majority of the work was a commercial heat of Ti–10V–2Fe–3Al obtained from Reactive Metals Incorporated. The chemistry of the heat was reported by the melters as:

Element	V	Al	Fe	N	C	O	Ti
Weight per cent	9.3	3.2	1.8	0.01	0.03	0.082	balance

The β-transus temperature of the primary material ingot was metallographically determined as 800°C. The starting condition of all test material in this study was obtained by β solution treating and water quenching the as-received conditioned ingot. Solution treatment was done by heat treating at 850°C for 30 min in either argon or in evacuated quartz capsules. Specimens were wrapped in zirconium foil during solution treatment to minimize oxidation, and specimen shapes were always machined prior to solution treatment to eliminate residual machining stresses.

Specimens were prepared for optical microscopy and X-ray analysis by electropolishing at room temperature in a 94% methanol + 5% sulfuric acid + 1% hydrofluoric acid solution. Thin foils for transmission electron microscopy were thinned in a 95% methanol + 5% sulfuric acid solution at −50°C. The elec-

tron microscopy itself was done with a JOEL 200CX. The X-ray tests were done on a modified Siemens diffraction goniometer using Cu–$K_{\alpha 1}$ radiation. All X-ray intensities reported in Tables 1 and 2 are normalized to the integrated peak heights of all shown peaks. Hot stage X-ray diffraction experiments were performed in an aluminum holder capable of heating a 7 mm diameter cylindrical specimen to 300°C in less than 3 min, and holding the set temperature to within 3°C. A silicon single crystal was used as the front face of the holder to eliminate the extraneous reflections from the holder, and to provide sharp calibration peaks. Neutron diffraction was used to supplement the X-ray tests since neutrons sample a much larger volume than do X-rays, and early tests showed that X-ray results were extremely sensitive to surface preparation. Neutron diffraction specimens were 15 mm in diameter, 30 mm in height, and were tested with the tensile axis perpendicular to the beam direction. Testing was done at the Institut für Reaktortechnik in Würenlingen, Switzerland, using neutron wavelengths of 2.335 Å.

Tensile strains were measured via clip-gauges during deformation, and monitored during reversion by either a dilatometer, or by measuring the migration of scribe marks with an optical measuring microscope.

Two dilatometers were used in this work. For the lower temperatures, a Netzch dilatometer modified to improve low temperature accuracy was used with a heating rate of 8°C per minute; for higher temperatures, a Cluesener dilatometer with heating rates of 3°C per min was used. In both cases, heating was done in a protective atmosphere.

RESULTS

The results of this investigation are presented below in five parts: the solution treated condition, the martensitic condition, martensite reversion and the shape memory effect, the reversion to alpha and isothermal reverse memory, and finally, the reversion of alpha back to beta.

The solution treated condition

Of the six heats of Ti–10–2–3 that were examined in this study, only one showed any evidence at all of a martensitic transformation after quenching from the solution treatment temperature. There are, however, two stipulations to this statement: firstly, the quenched specimens had to be kept quite thin so that quenching strains were minimized, and secondly, the specimens had to be electropolished to eliminate stresses which can occur during mechanical polishing. If either of these conditions were violated, a partially martensitic microstructure was found. Figure 1a shows a typical completely retained β microstructure; the grains are equiaxed, without a substructure, and are studded with small inclusions which appear to be based on a Ti_4P compound [20]. The material heat which did show some evidence of athermal or quenching martensite showed only inconsistent patches of martensite, preferentially residing at the grain boundaries, as illustrated in Fig. 1b.

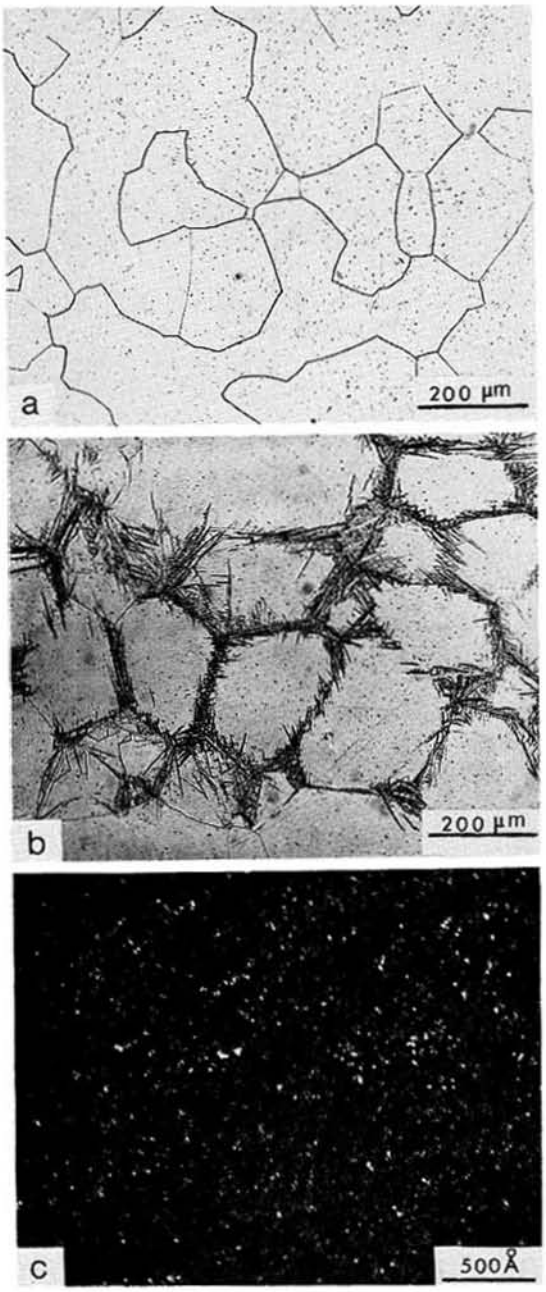

Fig. 1. Microstructure of the β solution treated and quenched material, (a) typical optical micrograph, (b) athermal martensite on grain boundaries, and (c) dark field of the athermal ω.

Transmission Electron Microscopy (TEM) showed that all heats contained very fine dispersions of athermal ω particles (designated ω_A). The particles, as shown in Fig. 1c, were 10 to 25 Å in diameter, irregularly shaped, and were accompanied by streaking on the $\langle 111 \rangle$ planes of the reciprocal lattice [20]. In the one ingot in which athermal martensite was found

Table 1. Neutron and X-ray diffraction results for five different conditions of Ti–10V–2Fe–3Al

β-ST + quenched					+2% Deformation					+Heating to 250°C					+Heating to 460°C					+Heating to 620°C				
Plane (1)	$\frac{\lambda}{2\sin\theta}$ (2)	I_N (3)	$I_\perp$ (4)	$I_\parallel$	Plane	$\frac{\lambda}{2\sin\theta}$	I_N	$I_\perp$	$I_\parallel$	Plane	$\frac{\lambda}{2\sin\theta}$	I_N	$I_\perp$	$I_\parallel$	Plane	$\frac{\lambda}{2\sin\theta}$	I_N	$I_\perp$	$I_\parallel$	Plane	$\frac{\lambda}{2\sin\theta}$	I_N	$I_\perp$	$I_\parallel$
α'' 110	2.57	—	—	1	α'' 110	2.57	5	8	—	α'' 110	2.56	—	1	2	α 020	2.54	4	3	7	α 020	2.539	—	4	13
α'' 020	2.45	—	4	1	α'' 020	2.45	—	—	55	α'' 020	2.45	—	—	4	α 002	2.32	12	20	10	α 002	2.336	8	16	9
α'' 002	2.32	—	4	1	α'' 002	2.32	—	1	—	α'' 002	—	—	—	—	β 111	2.28	42	3	35	β 111	2.277	43	46	33
β (5) 111	2.29	76	74	77	β 111	2.29	37	12	14	β 111	2.28	70	40	61	α 111	2.23	35	67	37	α 111	2.232	35	24	19
α'' 111	2.25	14	20	8	α'' 111	2.24	44	25	16	α'' 111	2.24	10	50	24	α 112	1.72	8	4	3	α 112	1.719	4	3	5
α'' 021	2.18	3	—	8	α'' 021	2.17	—	3	7	α'' 021	2.17	—	4	2	β 200	—	—	—	—	β 200	1.611	4	4	14
α'' 112	1.72	—	—	1	α'' 112	~1.71	5	9	—	α'' 112	1.72	10	2	2	α 200	1.47	—	1	5	α 200	1.467	6	1	3
α'' 022	1.69	—	—	2	α'' 022	1.68	—	1	1	α'' 022	1.68	10	—	2	$a = 2.93$	α-phase $b = 5.08$		$c = 4.67$		$a = 2.933$	α-phase $b = 5.078$		$c = 4.671$	
β 200	1.62	7	—	1	β 200	1.62	4	—	1	β 200		—	—	—	$a = 3.22$	β-phase $b = 4.55$		$c = 4.55$		$a = 3.221$	β-phase $b = 4.556$		$c = 4.556$	
α'' 200	1.51	—	—	—	α'' 200	1.51	5	36	—	α'' 200	1.50	—	2	2										
α'' 130	1.44	—	—	2	α'' 130	1.44	—	4	5	α'' 130	1.43	—	1	1										
$a = 3.01$	α''-phase $b = 4.91$		$c = 4.63$		$a = 3.01$	α''-phase $b = 4.91$		$c = 4.63$		$a = 3.01$	α''-phase $b = 4.91$		$c = 4.63$											
$a = 3.24$	β-phase $b = 4.58$		$c = 4.58$		$a = 3.24$	β-phase $b = 4.58$		$c = 4.58$		$a = 3.22$	β-phase $b = 4.55$		$c = 4.55$											

(1) Indexed in orthorhombic coordinates.
(2) Measured d-spacing in Angstroms.
(3) Neutron intensity ($\lambda = 2.335$ Å).
(4) X-ray intensities normal and parallel to tensile direction.
(5) Would be indexed as (110) in b.c.c. indexing system.

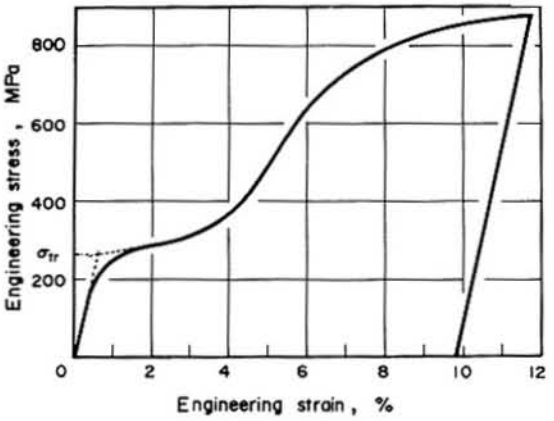

Fig. 2. Typical stress–strain curve for as-quenched Ti–10V–2Fe–3Al.

optically, the martensite could not be observed by TEM due to the thin foil relaxation problems described elsewhere [21].

Both X-ray diffraction and neutron diffraction were used to measure the lattice parameter of the retained β phase; the "best fit" value was determined as 3.24 Å. No indications of the hexagonal α or ω phases were found by these techniques. These diffraction results are summarized with the results from other conditions in Table 1. One should note that all phases are indexed as orthorhombic in Table 1. The reason for this should become clear upon reading the "Discussion" section of this paper. The apparently high α'' content shown in Table 1 is presumed due to quenching strains, since the specimens were quite large.

Specimens in the as-quenched condition were cooled in a dilatometer to see whether martensite could be formed. No deviation from the normal linear contraction of the β phase could be observed down to temperatures of -170°C, which represents the lowest temperature which the equipment can measure. In the one case where athermal martensite was observed, a specimen was also heated in the dilatometer to 200°C,

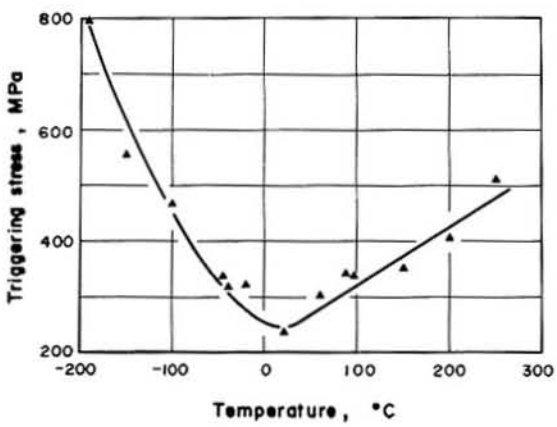

Fig. 3. Triggering stress plotted as a function of temperature.

Fig. 4. Microstructure after 2% plastic deformation.

again without deviation from linearity. These results imply, then, that the volume fraction of *athermal* martensite cannot be affected by temperature changes between -170° and 200°C.

Stress induced martensite

Tensile specimens tested in the solution treated and quenched condition all exhibited a "strain plateau" (shown in Fig. 2). The stress required to induce this strain plateau will be henceforth referred to as the "triggering stress", and will be defined as the intersection of the elastic modulus tangent and the tangential extension of the strain plateau slope (as illustrated in Fig. 2). Triggering stresses ranging from 180 to 450 MPa were found depending upon which heat was being tested. The heat showing the minimum average triggering stress, with a mean value of 220 MPa, was the heat which exhibited occasional evidence of athermal martensite. Over 30 specimens from this heat were pulled in this study, with triggering stresses ranging from 180 to 280 MPa. Since martensite was more easily induced in this heat than in the others, this heat was chosen as the primary heat in the shape memory and reversion studies reported below.

Tensile tests were also conducted at temperatures other than 20°C, and the triggering stress plotted as a function of temperature. The results (Fig. 3) show a distinct minimum triggering stress at ~20°C.

Investigations of microstructures after a few percent deformation confirmed that martensite had been formed during the deformation, as is shown in Fig. 4. Extensive attempts were made to study the martensite by TEM; unfortunately these attempts were largely unsuccessful due to the reversion of the martensite during the thinning process. Although some marten-

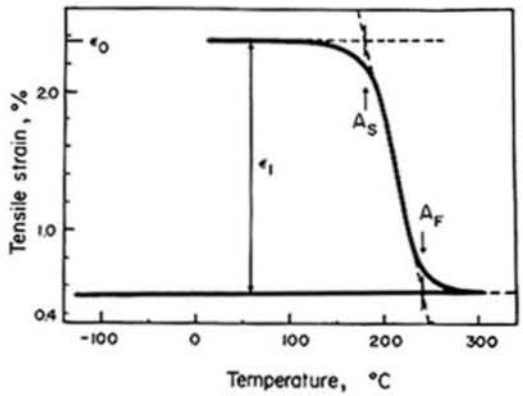

Fig. 5. Dilatometer output showing shape memory recovery after a tensile deformation of 2.4%, with a heating rate of 8°C per min.

site plates did survive thinning and were photographed, they are not shown here. Examples are shown elsewhere [7], but since the plates which are observable after thinning are atypical (the majority revert) one must question the statistical value of studying the plates in any detail. Athermal ω_A was uniformly found in the thin foils, but it should be pointed out that this is not proof that ω_A existed inside the martensitic plates prior to thin foil thinning; the ω_A may have precipitated during thinning after the martensite refersion. One observation which would seem valid, however, is that $\langle 111 \rangle \{112\}$ β twins were formed in the matrix during deformation [7].

Both X-ray and neutron diffraction confirmed that the martensitic structure was orthorhombic (designated α'') and that after 2.5% strain, the $\beta \rightarrow \alpha''$ transformation was incomplete. The α'' lattice parameters were determined as

$$a = 3.01\,\text{Å}$$

$$b = 4.90\,\text{Å}$$

$$c = 4.63\,\text{Å}.$$

X-ray tests were conducted with the beam direction

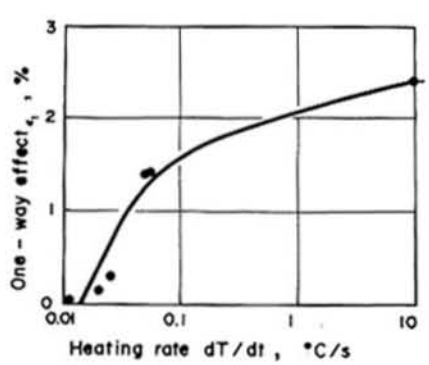

Fig. 6. Percent shape recovery as a function of heating rate after 2.5% tensile deformation.

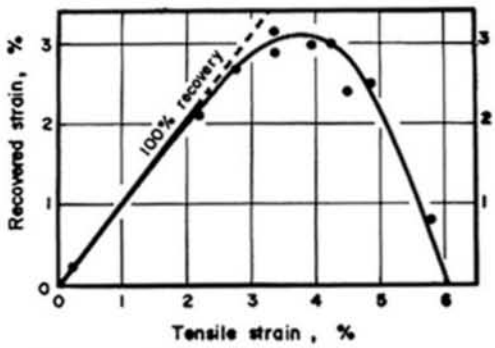

Fig. 7. Per cent shape recovery plotted as a function of initial tensile strain, with heating done in molten salt.

both parallel to and perpendicular to the tensile axis. As one should expect, the peak intensities were notably different in these two directions (see Table 1).

Martensite reversion and the shape memory effect

Gauge length sections were cut out of several deformed tensile specimens and heated in a dilatometer to 250°C at a rate of 8°C per minute, while continuously measuring length changes. During heating the specimens were found to contract to their lengths prior to deformation following the strain–temperature path shown in Fig. 5. Henceforth, the temperature at which a specimen begins to recover its shape prior to deformation will be termed the austenitic start temperature (A_s), and the temperature at which the recovery is completed will be termed the austenitic finish (A_F); both values are defined by a tangent construction, as shown in Fig. 5. A statistical survey of over 30 specimens resulted in an average A_s value of 166°C and an A_F value of 241°C, though a large scatter was noted. After heating to 250°C, the elements were cooled down while monitoring the strain. The shape recovered during heating was found to be permanent with very little, if any, two-way or reverse shape change occurring during cooling.

The magnitude of the shape recovery, or shape memory effect, was found to be dependent on both

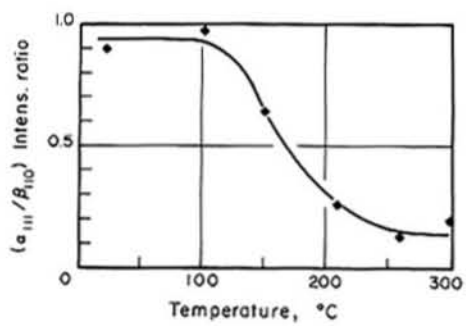

Fig. 8. Results of hot stage X-ray diffraction work showing the relative intensity ratio of the α''-(111) and the β-(110) reflections as a function of temperature; original deformation was 2.5%.

Table 2. Comparison of X-ray spectrums after heating in a salt bath and in a furnace.

Plane†	$2 \sin \theta/\lambda$‡	I (salt)§	I (air)¶
α'' (110)	2.57	—	4
β (111)	2.28	93	86
α'' (111)	2.24	—	9
β (200)	1.59	7	1

† Plane indices in orthorhombic system.
‡ Measured d-spacing in Angstroms.
§ Intensities after rapid heating to 275°C.
¶ Intensities after slow heating to 275°C.

heating rate and the magnitude of the original tensile strain. The dependence upon heating rate was measured by fixing the tensile strain at 2.5% and changing the dilatometer heating rate (Fig. 6). (The most rapid heating rate shown in this figure was obtained by measuring specimen length before and after immersion into a 250°C salt bath.) The results demonstrate that the maximum memory effect is obtained by heating as rapidly as possible. The influence of initial strain on the completeness of shape recovery was measured by choosing the fastest possible heating rate (immersion in salt) and varying the tensile strain. The results (Fig. 7) show that perfect recovery is possible after strains of 3% or less; above 5%, the memory effect disappears quite quickly.

After heating in the dilatometer to 250°C and cooling, some of the deformed tensile gauge sections were sectioned for analysis. X-ray diffraction showed that both the β and the α'' phases were still present (Table 1), but that the α'' reflections were not as strong as they were prior to heating. Again no signs of the α or the ω structures were found. Neutron diffraction gave similar results. Hot stage X-ray diffraction work was done to verify that the structure after cooling from the dilatometer temperature is indeed the same as that prior to cooling. The reflections at 250°C were essentially identical to those after cooling, and thus it can be inferred that no transformation was occurring during cooling. Figure 8 shows some of the results of these hot stage experiments. Here the intensities of the β and the α'' peaks are plotted as a function of temperature. Note that the shape of the curve is quite similar to that produced by the dilatometer, shown in Fig. 8.

To help understand the role of heating rate on reversion and shape memory, two specimens of a heat showing no α'' in the β-ST'ed and quenched condition were deformed and then heated to 275°C, one in a salt bath, and the other in a box furnace. The specimens were then sectioned and X-rayed. The results, shown in Table 2 clearly demonstrate that the $\alpha'' \rightarrow \beta$ reversion is severely hindered by slowly heating to A_F.

Optical microscopy verified that a martensitic structure was still present and that the reversion of α'' to β was largely incomplete (Fig. 9a). Thin foil relaxation was not as prevalent as in the undeformed condition, and thus it was possible to examine the martensite via TEM. Figures 9b and c respectively show dark field images of the α'' and β phases. The microstructure appeared to consist of lamellae alternating between α'' and β. The α'' shown in Fig. 9b had a striated internal structure, while the modulations in the β plates were shown to arise from isothermal ω precipitation (shown more clearly in Fig. 9d).

Reversion to α and isothermal reverse memory

Instead of cooling after reaching 250°C, some specimens were left in the dilatometer and heated further. A typical strain–temperature result is shown in Fig. 10. As is shown, there is a *reverse shape memory movement* during the continued heating. In order to determine whether or not this reverse memory effect was isothermal or athermal, some isothermal aging experiments were conducted. Gauge lengths from deformed tensile specimens were removed and placed in 450°C salt for various times ranging from 10 to 50,000 s. Specimen lengths were measured with a micrometer before and after immersion. The resulting aging curves are shown in Fig. 11. A large recovery of the original undeformed shape was observed during the first 10 s; further aging resulted in a partial recovery of the deformed shape roughly following an erf(T) type of behavior. The magnitude of the original strain was also critical—specimens strained less than 2% showed a permanent one-way effect (no reverse movement), and specimens strained above 5% showed no one-way effect and no reverse movement. Another very important point can be made by comparing Figs 10 and 11. The rate of heating to the aging temperature is apparently important; the slower heating rates of the dilatometer (Fig. 10) produced larger reverse recovery effects than were found when the same strain level was tested by rapidly heating in a salt pot (Fig. 11).

After heating in a dilatometer to 460°C, a specimen was removed, cooled quickly, and sectioned for diffraction studies and metallography. X-ray analysis showed an entirely β plus α structure, as is shown in Table 1. Optically, the microstructure appears to be quite similar to that found after 250°C, except that the volume fraction of coarse plates is lower (Fig. 12a). Finding the coarse α plates by TEM was difficult in this condition. Plates that were found appeared similar to that shown in Fig. 9b and c. The fine omega structure was still observed, but now mixed with very fine, highly acicular α plates (Fig. 12b).

Reversion of the α back to β

When dilatometer heating was continued past 450°C, several more shape adjustments were observed (Fig. 13). In order to make sure that the dilatometer was operating correctly and that these adjustments were, in fact, real, a specimen was deformed in compression and tested in exactly the same manner. The curves for both deformation senses are shown in Fig. 13—the heavy line being the tension curve and the

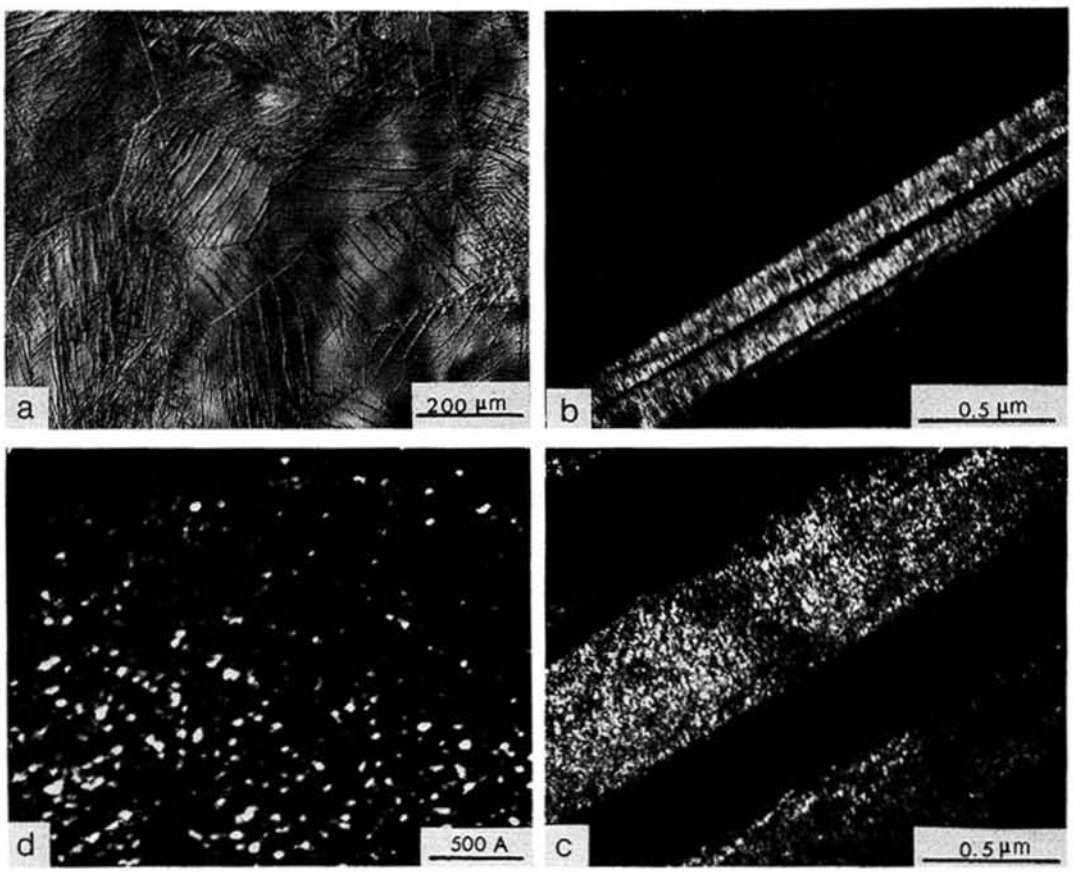

Fig. 9. Microstructure of 10–2–3 after deformation and subsequent slow heating to 250°C. Shown are an (a) optical micrograph, (b) TEM micrograph dark field using a α''-(111) reflection, (c) dark field TEM micrograph of the same area using a β-(110) reflection, and (d) dark field showing isothermal ω particles.

lighter line being the compression curve. The magnitude of the various shape adjustments are not the same since the tension specimen was originally longer than the compression specimen, but both the senses and the temperatures of the various shape adjustments were quite reproducible.

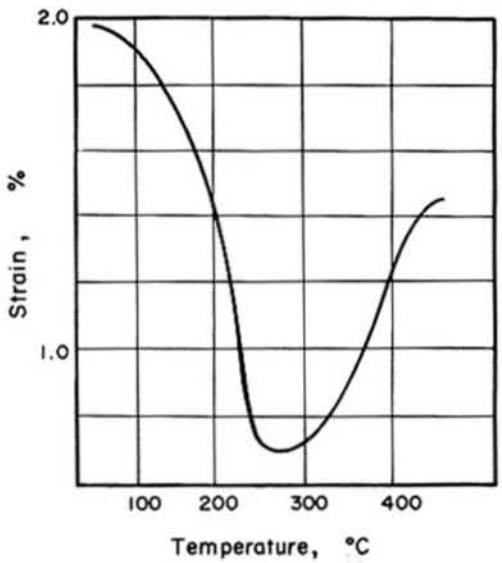

Fig. 10. Dilatometer output illustrating the one-way shape memory effect and the reverse two-way memory effect; heating rate was 3°C per min.

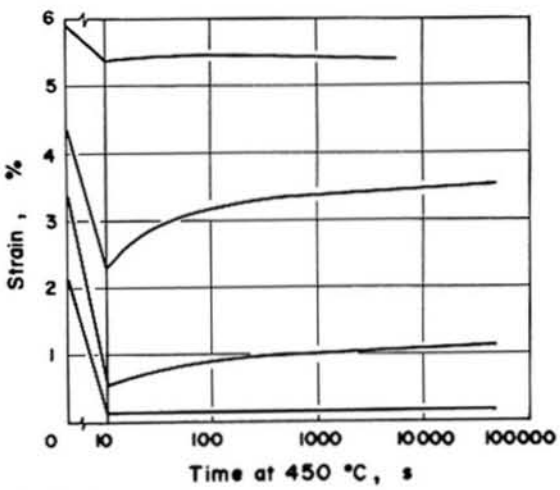

Fig. 11. Isothermal aging curves showing the isothermal nature of the reverse memory effect at several strain levels. The first data point (after 10 s) represents the usual one-way effect and perhaps the earliest part of the reverse effect.

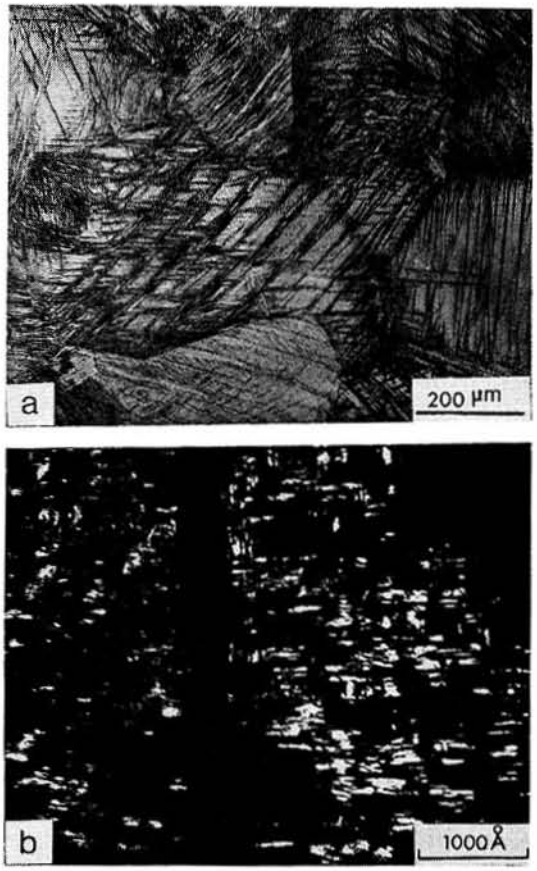

Fig. 12. Microstructure after slowly heating to 460°C, shown (a) optically, and (b) by a TEM dark field of overlapping α and ω reflections.

One specimen was removed from the dilatometer for microscopic analysis when a temperature of 650°C was achieved. The microstructure was found to be $\beta + \alpha$, with the α being entirely in the form of extremely fine platelets visible optically only as modulations. Since coarse α plates could not be found via TEM, the plates shown in Fig. 14 are assumed to be only β-twins. X-ray analysis showed sharp $\beta + \alpha$ reflections (Table 1) with the reflections being much narrower than those previously found.

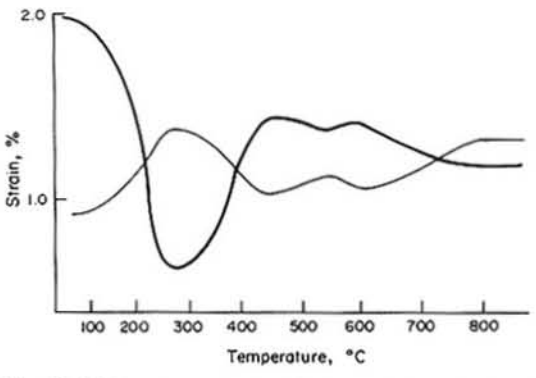

Fig. 13. Dilatometer outputs after tensile (heavy line) and compressive (narrow line) deformations; the strain scale corresponds only to the tensile curve.

Fig. 14. Optical micrograph showing microstructure after deformation (2.5%) and slowly heating to 620°C.

DISCUSSION

The results presented in the previous section are best understood when both the b.c.c. and the h.c.p. structures are visualized by alternate, but fully equivalent, representations; more specifically, the b.c.c. structure should be visualized by a face centered tetragonal cell, and the h.c.p. structure by an orthorhombic symmetry. The equivalence of these 'thought transformations' is illustrated in Fig. 15. Throughout the discussion which follows, both the α and β phases will be referred to and notated in terms of these alternate structural cells unless specifically noted otherwise. As a further simplification, the β phase will be referred to as "orthorhombic", even though it can be reduced to a tetragonal symmetry by virtue of its two equal lattice parameters. The validity and the value of these representations are, to some extent, pointed out by considering the Burger's α–β orientation relationship

$$(110)_{\beta}^{\text{b.c.c.}} \parallel (0001)^{\text{h.c.p.}}$$

$$[111]_{\beta}^{\text{b.c.c.}} \parallel [11\bar{2}0]_{\alpha}^{\text{h.c.p.}} \text{ (approximate).}$$

These same transformations, when expressed in terms of the proposed *orthorhombic representations* become simply

$$(001)_{\beta} \parallel (001)_{\alpha}$$

$$[110]_{\beta} \parallel [110]_{\alpha} \text{ (approximate).}$$

Indeed the Burger's $\beta \rightarrow \alpha$ transformation itself can be visualized now as a simple adjustment of the β orth-

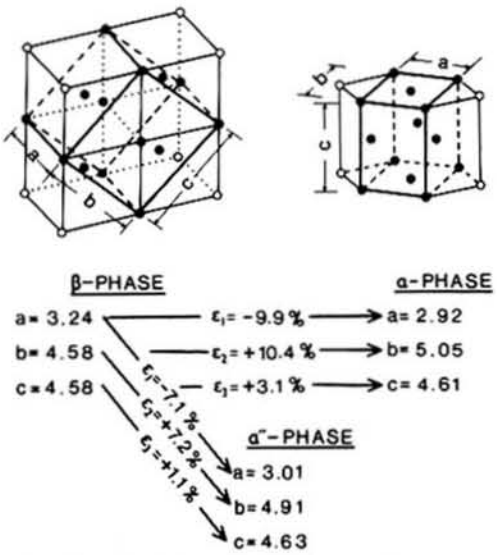

Fig. 15. Orthorhombic representations of the α and β phases. The original h.c.p. and b.c.c. structures are depicted by narrow lines and open circles, while the orthorhombic cells are depicted by heavy lines and closed circles. The lattice parameters and lattice strains of the orthorhombic cells were measured via X-ray diffraction except in the case of the α-phase, where the parameters were calculated assuming no change in specific volume during the $\beta \rightarrow \alpha$ transformation.

orhombic structure; in the ideal case, with no change in specific volume, this transformation consists of the following cell distortions

$$a_\beta \rightarrow a_\alpha$$

$$b_\beta = \sqrt{2}a_\beta \rightarrow b_\alpha = \sqrt{3}a_\alpha$$

$$c_\beta = \sqrt{2}a_\beta \rightarrow c_\alpha = 1.59a_\alpha$$

with the following atomic shuffles

$$(0,0,0)_\beta \rightarrow (0,0,0)_\alpha$$

$$(a/2,b/2,0)_\beta \rightarrow (a/2,b/2,0)_\alpha$$

$$(0,b/2,c/2)_\beta \rightarrow (0,2b/3,c/2)_\alpha$$

$$(a/2,0,c/2)_\beta \rightarrow (a/2,b/6,c/2)_\alpha.$$

Following this system of thought, the orthorhombic structure can easily be visualized as an incomplete progression of the $\beta \rightarrow \alpha$ reaction, or as a compromise structure—an orthorhombic structure with lattice parameters lying between those of α and β, parameters which do not permit the cell to be reduced to a higher order of symmetry as is the case with α and β. One can express this in another way by stating that *the lattice strains* (ϵ_1, ϵ_2 and ϵ_3) *needed to form the* α *structure from* β *are identical in sense but larger in magnitude than the strains needed to form* α". This point is numerically made clear by Fig. 15.

With the above background, the results presented in the previous section will be discussed. For the sake of symmetry, the discussion will be subdivided as in the previous section.

The solution treated structure

The M_s line on most beta stabilized phase diagrams is quite steep at room temperature (see, for example, [13]). Thus it becomes proper to talk in terms of a critical compositional limit for martensite formation. The alloying elements present in Ti–10–2–3 would seem to place the alloy just to the right of that limit; so close, in fact, that exceptional care in sample preparation was necessary to prevent a stress-assisted surface decomposition of β to α". One of the heats used in this study showed martensite at the grain boundary even when extensive precautions were taken to preserve the quenched β structure. Clustering of martensite at the grain boundaries such as is shown in Fig. 1b could be due to the accommodation of quenching strains, or more simply, due to the enhancement of nucleation at the grain boundary.

Stress induced martensite

Stresses of only 220 MPa were necessary to induce the $\beta \rightarrow \alpha''$ martensite reaction. Based on Fig. 15, one can see that the β to α" transformation is accompanied by lattice strains in the three principal lattice directions of $\epsilon_1 = -7.1\%$, $\epsilon_2 = +7.2\%$ and $\epsilon_3 = +1.1\%$. Since the specific volumes of the α" and the β structures are identical, an applied stress simply stabilizes those martensite variants which best accommodate the applied stress. As an example, we can consider a tensile test. If, after deformation, one were to look at the crystal planes on a cross section perpendicular to the tensile axis, one would expect to see no $(200)_\alpha$- planes after the deformation since ϵ_1 is negative during the $\beta \rightarrow \alpha''$ adjustment. Similarly, one would expect quite strong reflections from the $(020)_\alpha$-planes, since ϵ_2 increases during the transformation and is thereby stabilized by a tensile stress. With the beam direction perpendicular to the tensile axis, one would expect to see plane reflections whose normals undergo negative lattice strains (such as the $(200)_\alpha$- and the $(101)_\alpha$- planes), and to see only very weak reflections from planes whose normals undergo positive strains (such as the $(020)_\alpha$- and $(022)_\alpha$- planes). Although a more exact prediction of a deformed α" texture is complicated by the initial material texture, the reader should confirm the validity of the above predictions by examining the intensity variations in the 2% deformed material shown in the second division of Table 1.

Unfortunately thin foil relaxation effects prevented a detailed study of the internal martensite structure. One should note, however, that ω_A was observed. Although it cannot be stated with confidence that the ω_A was present within, or even along with, the α", it is clear that the ω_A was present *prior* to the deformation. Thus the α" structure was formed from $\beta + \omega_A$, not just β. There are two obvious ways for this to occur. The first is if the ω_A particles are dissolved before the α" interface advances through the $\beta + \omega_A$ matrix, and the second is if the particles can be

sheared along with the β directly into the α'' structure. Unfortunately we have no direct evidence for either.

The extremely large discrepancy between A_s (166°C) and M_s (below −170°C) may be indicative of a high activation energy for the movement of the α'' interface. But perhaps more to the point is the unusual triggering stress vs temperature plot shown in Fig. 3. An increase in triggering stress with increasing temperature is expected, since the martensite is becoming continuously less stable and more difficult to stress 'induce'. What is more unusual, is the sharp stress increase with decreasing temperatures. The dilemma here is that as temperatures are reduced, the martensite is surely becoming more stable with respect to the β phase, and thus the triggering stress should continue to decrease with temperature. One possible explanation for this unusual behavior comes from the ω_A particles. These ω_A particles also become more stable as temperature is reduced [22]. If the ω_A particles must be reverted to β prior to the advancement of an α''–β interface, we would expect decreasing temperatures to make the α'' inducement more difficult, and thus the triggering stress to increase.

The reversion of α'' to β and the shape memory effect

The highly oriented α'' found after deformation is reverted to β upon heating above A_s (166°C), and in the process, the material returns to its shape prior to deformation. This reversion can be assumed to be an athermal shearing process, since the memory improves as the heating rate is increased (Fig. 6), and, more directly, because X-ray results presented in Table 1 indicated that the $\alpha'' \rightarrow \beta$ reaction is more complete when faster heating rates are used. Further, the fact that the α'' phase is stabilized by slower heating rates is indicative that the α'' plates are becoming leaner in Fe and V via diffusional processes. Similar behavior has been observed in other systems, at higher temperatures [15]. Unfortunately, due to the broad, spread-out nature of the α'' reflections, it was not possible to see an expansion of the α'' lattice which would have been indicative of Fe and V depletions. The β lattice parameter was found to decrease slightly, but this could simply be reflective of Fe and V enrichment from the precipitation of ω.

In addition to the athermal $\alpha'' \rightarrow \beta$ reaction, and the diffusional stabilization of the remaining α'' plates, there is an $\omega_A \rightarrow \omega_I$ transformation occurring in the β matrix. Thus we can summarize the transformations occurring during the eary stages of reversion as follows

$$\alpha'' \rightarrow \beta \text{ (athermal)}$$

$$\alpha'' \rightarrow \alpha''_{\text{lean}} \text{ (isothermal)}$$

$$\omega_A \rightarrow \omega_I \text{ (isothermal).}$$

Clearly the first two transformations compete directly with one another, with faster heating rates favoring the first.

Transformation to α and isothermal reverse memory

The two reactions that were found to occur during the later stages of reversion were

$$\alpha''_{\text{lean}} \rightarrow \alpha$$

$$\beta + \omega_I \rightarrow \beta + \alpha$$

The second reaction shown above gives rise to very fine, uniform α plates, and cannot be responsible for the isothermal shape memory effect described in the previous section. The first reaction, however, could produce a memory effect. From Fig. 15, one can see that the lattice strains introduced by the α phase are simply an exaggeration of the strains introduced by the α'' phase. *Thus whatever strains are stored in the unreverted diffusionally stabilized α'', are exaggerated when the α'' structure is transformed into α.* In principle, one could even imagine a reverse memory effect returning a shape beyond that of the original deformation.

The observation that slower heating rates yield larger reverse memory effects supports the above proposal, since the slower heating rates transformed less of the α'' back to β athermally, and left more α''_{lean} plates behind to transform to α. Similarly, the low strain levels, which tend to revert quite completely to β, produced the lowest reverse memory (Fig. 11). The highest strain levels of Fig. 11 are associated with extensive dislocation movement, and would therefore not be expected to produce either a memory effect or a reverse memory effect.

The reversion of α back to β

As the β-transus temperature (800°C) is approached, the α phase begins to dissolve, and thus all strains stored in the selective α plate variants are lost. Thus a third shape change is expected. This last shape change should be largely athermal, since the equilibrium α/β volume fractions are quite quickly established at these high temperatures. What was found (Fig. 13), however, was not a simple, monotonic shape recovery. A dip in the strain–temperature curve was observed at 530°C, followed by a continued recovery of the deformed structure. The origin of these last shape 'adjustments' is not clear. One could speculate that the reverse memory effect has its maximum at 600°C, and that the dip shown 530°C was due to a dislocation recovery process. This speculation would reflect, however, simply the most plausible of several implausible explanations, supported only by the observation that the α and β peaks became notably sharper between the two maximums.

SUMMARY

The formation and reversion behaviors of stress induced orthorhombic martensite has been studied in Ti–10V–2Fe–3Al, and can be summarized as follows:

$\beta + \omega_A (+\alpha'')$	(The starting microstructure. The α'' martensite being found only in poorly prepared specimens, and occasionally in unusually 'lean' heats.)
$\beta + \omega_A \rightarrow \alpha''$ (stress assisted)	(Triggered by stresses of 220 MPa or higher, with the 'induced' martensite structure 'storing' up to 5% deformation through the formation of preferred orientations.)
$\alpha'' \rightarrow \beta$ (athermal)	(Reshearing of α'' back to the original β orientations, resulting in a 100% one-way recovery of strains as high as 3%. The austenization temperatures were found to be $A_s = 166°C$ and $A_F = 240°C$.)
$\alpha'' \rightarrow \alpha''_{lean}$ $\omega_A \rightarrow \omega_I$ (isothermal)	(Two isothermal reactions taking place at very low temperatures, the first of which hinders the athermal $\alpha'' \rightarrow \beta$ reaction by stabilizing α'', presumably via depletion of Fe and V.)
$\alpha''_{lean} \rightarrow \alpha$ $\beta + \omega_I \rightarrow \beta + \alpha$ (isothermal)	(Two isothermal reactions which are essentially continuations of the previous reactions, both producing 'Burger's' α. The first reaction was found to produce a *reverse* shape memory effect, due to the increasing lattice strains associated with the continuous transformation from β to α'' to α.)
$\alpha \rightarrow \beta$	(The reversion of α back to β as the 800°C β-transus temperature is approached. This reaction was also accompanied by a 'shape memory effect', due to the reversion of the preferred α orientations.)

Several different investigative methods were employed during this study—in several instances, only in a cursory fashion. There are several questions which have not been satisfactorily addressed, such as: why is the α'' phase stabilized by slow heating rates? What happens to the ω_A particles as the α''–β interface advances? What is the internal structure of the α'' plates? What causes the final shape 'adjustments' as the β-transus temperature is approached. Clearly some detailed EDX-STEM work coupled with some more quantitative diffraction textural measurements would be useful in answering some of these questions.

REFERENCES

1. Y. C. Liu, *Trans. A.I.M.E.* **206**, 1036 (1956).
2. M. K. Koul and J. F. Breedis, *Acta metall.* **18**, 579 (1970).
3. M. J. Blackburn and J. C. Williams, *Trans. T.M.S.-A.I.M.E.* **242**, 2461 (1968).
4. T. S. Kuan, R. R. Ahrens and S. L. Sass, *Metall. Trans.* **6A**, 1767 (1975).
5. R. A. Wood *et al.*: AFML-TR-70-257 (1970).
6. C. Baker, *Metal Sci. J.* **5**, 92 (1971).
7. T. W. Duerig *et al.*, *Proc. Fourth Ann. Conf. on Titanium*, p. 1503 (1980).
8. R. W. Coade, T. W. Duerig and G. H. Gessinger, Effect of microstructure on the mechanical properties of transage 134, *Proc. Sixth Int. Conf. on the Strength of Metals and Alloys* (1982). To be published.
9. C. J. Williams, *Proc. Second Int. Conf. on Titanium*, p. 1433 (1972).
10. J. C. Williams and B. S. Hickman, *Metall. Trans.* **1**, 2468 (1970).
11. Y. Murakami, *Proc. Fourth Int. Conf. on Titanium*, p. 153 (1980).
12. R. Davis, H. M. Flower and D. R. F. West. *Acta metall.* **27**, 1041 (1971).
13. R. Davis, H. M. Flower and D. R. F. West, *J. Mater. Sci.* **14**, 712 (1979).
14. I. A. Magariatskii *et al.*, *Soviet Phys. Doklady* **3**, 1014 (1959).
15. M. Young, E. Levine and H. Margolin, *Metall. Trans.* **5**, 1891 (1974).
16. K. A. Bywater and J. W. Christian, *Phil. Mag.* **25**, 1275 (1972).
17. C. M. Wayman and K. Shimizu, *Metal Sci. J.* **6**, 175 (1972).
18. L. Delaey *et al.*, *J. Mater. Sci.* **9**, 1621 (1974).
19. T. W. Duerig, D. F. Richter and J. Albrecht, *Scripta metall.* In press.
20. T. W. Duerig, G. T. Terlinde and J. C. Williams, *Metall. Trans.* **11A**, 1987 (1980).
21. R. A. Spurling, C. G. Rhodes and J. C. Williams, *Metall. Trans.* **5**, 2597 (1974).
22. D. De Fontaine, N. E. Paton and J. C. Williams, *Acta metall.* **19**, 1153 (1971).